

## Research Article

# Study on the Imbibition Characteristics of Different Types of Pore-Throat Based on Nuclear Magnetic Resonance Technology

Xiong Liu <sup>1</sup>, Yang Zhang <sup>1</sup>, Ziming Zhang <sup>2</sup>, Jinze Xu <sup>1,3</sup>, Desheng Zhou <sup>1</sup>, Jian Su <sup>2</sup> and Ying Tang <sup>1</sup>

<sup>1</sup>School of Petroleum Engineering, Xi'an Shiyou University, Xi'an, China

<sup>2</sup>Drilling & Production Technology Research Institute, PetroChina Liaohe Oilfield Company, Panjin, China

<sup>3</sup>Department of Chemical and Petroleum Engineering, University of Calgary, Calgary, Canada

Correspondence should be addressed to Jinze Xu; jinzxu@ucalgary.ca

Received 14 November 2021; Revised 12 February 2022; Accepted 7 April 2022; Published 27 April 2022

Academic Editor: Andri Stefansson

Copyright © 2022 Xiong Liu et al. This is an open access article distributed under the Creative Commons Attribution License, which permits unrestricted use, distribution, and reproduction in any medium, provided the original work is properly cited.

“Fracturing network+imbibition oil production” is a new attempt to effectively develop low-permeability tight reservoirs. Fracturing fluid is not only a carrier for sand carrying but also a tool in the process of imbibition. On the basis of imbibition experiments, combined with nuclear magnetic resonance and pseudo-color processing technology, this paper clarified the dominant forces of different types of pore-throat and quantitatively characterized the contribution of different levels of pore-throat to imbibition oil recovery. The results show that gravity is the main controlling force of imbibition for reservoirs with higher permeability. Fluid replacement mainly occurs in the early period of imbibition. Macropores contribute most of the imbibition recovery, mesopores have a weak contribution, and the contribution of micropores and pinholes can be ignored. For the reservoirs with low permeability, capillary force is the main controlling force of imbibition. Fluid replacement mainly occurs in the later period of imbibition. Macropores contribute most of the imbibition recovery rate, mesopores contribute a small part of the imbibition recovery factor, and the contribution of micropores and pinholes can be ignored. This paper clarified that macropores and mesopores are the main sources of the contribution of imbibition recovery efficiency, and oil content and connectivity are key factors for the imbibition recovery efficiency.

## 1. Introduction

The development potential of low-permeability tight oil reservoirs is huge [1, 2], and imbibition oil recovery has become the most effective method for enhancing oil recovery for this type of oil reservoirs [3, 4]. Its principle is to use capillary force as the main displacement power to enhance the oil-water replacement capacity between fractures and rock matrix [5, 6]. It can finally achieve the purpose of increasing the degree of crude oil production in the matrix [7, 8]. It is significant to clarify the main controlling factors of different levels of pore-throat and analyze the imbibition characteristics of different types of pore-throat for improving the productivity of a single well [9–11].

At present, there are many scholars who study the law of imbibition oil production based on nuclear magnetic resonance technology: Mason et al. [12–14] compared the imbi-

tion characteristics of rocks under the different boundary conditions. The results show that the imbibition rate of rocks increases with the increase in the total surface area and the recovery increases with the increase in the rock shape factor. Bertonecello et al. took advantage of nuclear magnetic resonance technology to study the influence factors on imbibition [15, 16]. The results show that the greater the permeability and the longer the shut-in time, the higher the imbibition replacement efficiency; the higher the initial water saturation and the longer the imbibition equilibrium time, the lower the imbibition replacement efficiency; and the higher the permeability and injection ratio, the longer the imbibition distance [17–19]. Chen et al. evaluated the influence physical parameters on the dynamic imbibition efficiency [20, 21]. The results show that the average pore radius, permeability, porosity, average pore-throat ratio, medium diameter, average throat radius, and specific surface

TABLE 1: The physical parameters of cores.

Core number	Porosity (%)	The gas measurement permeability ( $10^{-3} \mu\text{m}^2$ )	Length (cm)	Diameter (cm)	Dry weight (g)
1	19.57	14.140	3.95	2.50	39.232
2	2.78	0.059	4.00	2.50	49.745

area are the main factors that affect the dynamic imbibition efficiency, and the degree of influence of those on the imbibition efficiency is gradually poor. The degree of influence of the sorting coefficient on the imbibition efficiency is relatively small [22, 23]. Liu et al. [24] conducted experiments on the imbibition characteristics of tight sandstone reservoirs through nuclear magnetic resonance and mercury intrusion porosity testing, which studied the pore-throat limit of imbibition, examined the relationship between pore throat and reservoir parameters, and proposed the imbibition mechanism of tight sandstone reservoirs. Oort et al. made a profound study on oil-water displacement under the action of osmotic pressure and capillary force in shale reservoirs [25, 26] and obtained the displacement characteristics of pore fluid in the process of imbibition [27, 28]. However, most of the above studies are on the mechanism and influencing factors of imbibition. It is basically a qualitative analysis, without clarifying the main control force of different types of pore-throat and without quantifying the contribution of different types of pore-throat to imbibition oil recovery. The innovations of this paper are as follows: based on the imbibition experiment of cores, combined with the technology of nuclear magnetic resonance and pseudo-color processing, this paper is aimed at achieving the purpose of clarifying the main controlling force of different types of pore-throat and quantitatively characterizing the contribution of different types of pore-throat to imbibition oil recovery.

## 2. Core Characteristics

In order to study the characteristics of different types of pores and throats, two cores with relatively different physical parameters were selected for experimental research. As shown in Table 1, the gas measurement permeability of core 1 is  $14.140 \times 10^{-3} \mu\text{m}^2$  and the porosity of core 1 is 19.57%, which belongs to the low-porosity and low-permeability core. And core 2 has a gas measurement permeability of  $0.059 \times 10^{-3} \mu\text{m}^2$  and a porosity of 2.78%, which belongs to the ultra-low-porosity and tight core.

Figure 1 shows the test results of core 1 and core 2 casting thin slices and scanning electron microscopy. Through the analysis, we can get the conclusion as follows: core 1 is mainly composed of siliceous self-formed filling pores, and the metasomatism of silty crystal dolomite is obvious. It mainly replaces volcanic rock debris. The feldspar and volcanic debris dissolve significantly. Kaolinite fills the pores with a small amount of metasomatic debris. Tuffaceous hydration is positive, and it exhibits wavy extinction characteristics under cross-lighting. The eruptive rock of core 1 accounts for 47%, and the total aperture ratio of core 1 is 7.0%. The pores are mainly intercrystalline pores and intergranular

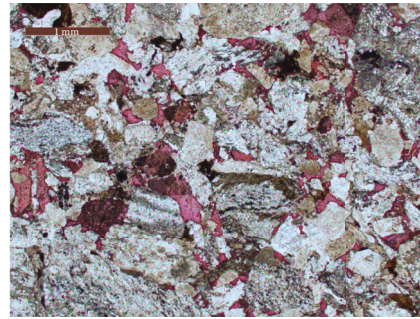
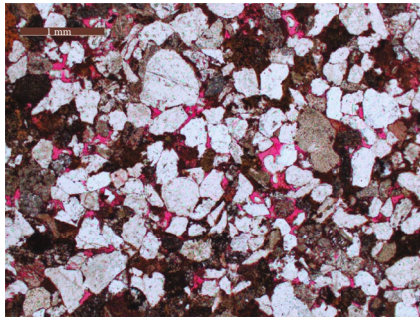
pores. The sorting is good. The pore type is mainly intergranular residual pores. The diagenesis authigenic minerals are composed of clay minerals such as kaolinite and are mostly produced in the form of pore filling; core 2 is mainly quartz schist and metamorphic quartzite cuttings. Its main component is iron calcite with a small amount of illite filling pores. The features of core 2 are poor pore development and poor sorting. Schist of core 2 accounts for 60%, and total porosity of it is 1.2%. The main types are residual pores and fissures between grains. The diagenetic authigenic minerals are composed of clay minerals such as iron mixed layer and illite and are produced in the form of pore filling and cushioning.

Figure 2 is a bar chart of the pore-throat distribution of the two cores. It can be seen that the peak of the pore-throat size distribution of core 1 is 2.5~6.3  $\mu\text{m}$ . Pore-throat size less than 0.1  $\mu\text{m}$  accounts for 17.96%, the pore size of 0.1~1.0  $\mu\text{m}$  accounts for 25.77%, and the proportion of the pore size more than 1.0  $\mu\text{m}$  is 56.27%. The quality of core 2 is poor, most of the pore-throat size is less than 0.1  $\mu\text{m}$ , and the proportion of pore-throat in this part is as high as 66.37%.

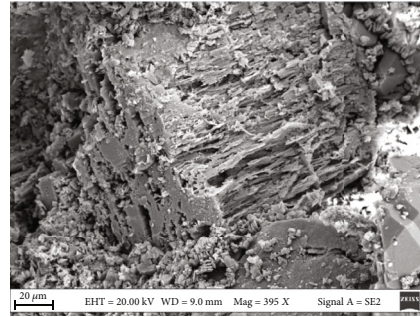
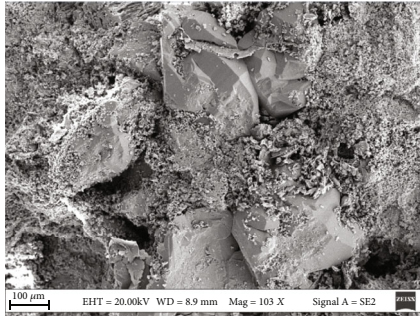
## 3. Experimental Process

This paper is based on the core imbibition experiments, combined with the technology of the nuclear magnetic resonance (MesoMR23-60H-I medium-size nuclear magnetic resonance spectrometer) and pseudo-color processing to study the imbibition characteristics of different types of pore-throat. The experimental process is as follows:

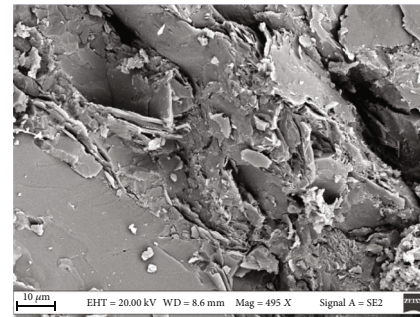
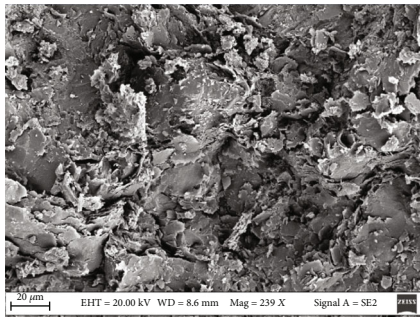
- (1) Cut core 1 and core 2 into small cores with a length of about 4.00 cm and a diameter of 2.50 cm; then, clean them simply and maintain the original wettability
- (2) Place the core in the displacement device and pressurize it to displace saturated distilled water until it is fully saturated; then, let it stand for a period of time; perform the first NMR scan with a nuclear magnetic resonance instrument on the core, and record the core signal when it is fully saturated with distilled water
- (3) Use fluorine oil to reversely drive the saturated core until no distilled water is produced. The fluorine oil used meets the condition of no nuclear magnetic signal. Let it stand for a period of time to ensure that the core fluid is fully balanced under the action of capillary force. Then, perform the second NMR scan with an MRI machine on the core to record the core signal after reverse saturation of fluorine oil



(a) Casting thin section of the core (intergranular pores and dissolved pores) (b) Casting thin section of core 2 (overall dense)



(c) Scanning electron microscope of core 1 (intergranular pores) (d) Scanning electron microscope of core 1 (detrital particles, dissolved pores)



(e) Scanning electron microscope of core 2 (intergranular residual pores) (f) Scanning electron microscope of core 2 (intergranular flake illite)

FIGURE 1: Cast thin section and scanning electron microscope.

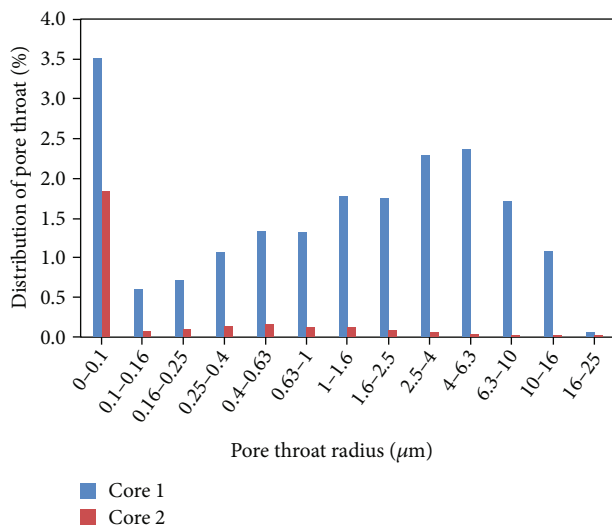


FIGURE 2: The pore-throat distribution of the core.

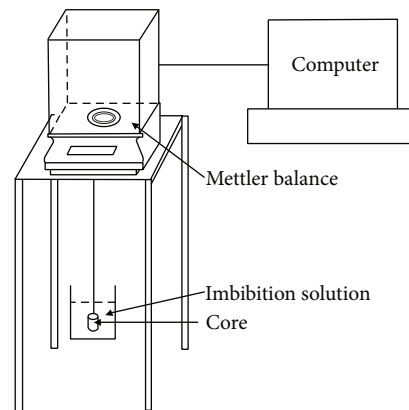


FIGURE 3: Self-imbibition experimental device.

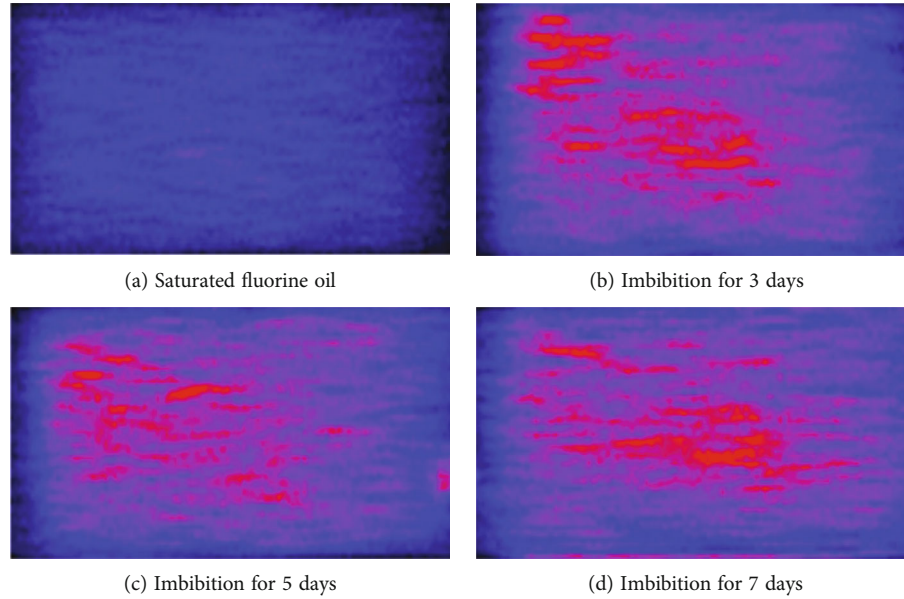


FIGURE 4: Pseudo-color image of core 1 (red is the water phase signal).

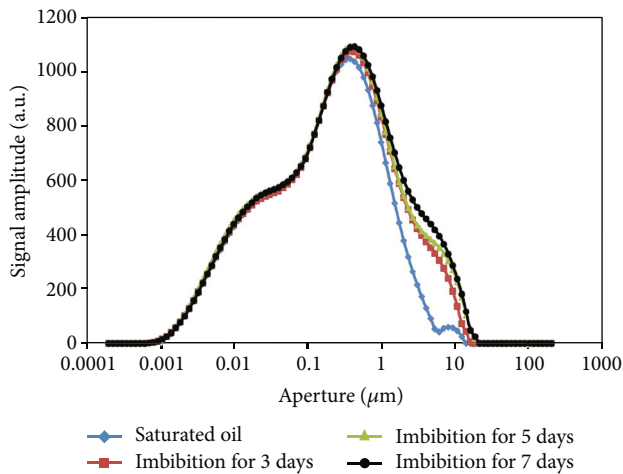


FIGURE 5: NMR T2 spectrum curve of core 1.

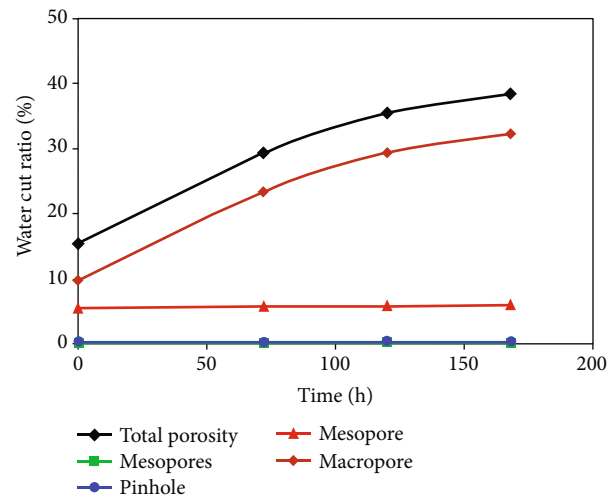


FIGURE 6: Variation curve of water cut of different types of pore-throat in core 1 with imbibition time.

- (4) The core self-imbibition experiment system is constructed as shown in Figure 3. The core saturated with fluorine oil was suspended vertically in the distilled water imbibition liquid, and the core is taken out after the imbibition for 3 days, 5 days, and 7 days. Then, the core was subjected to resonance scanning, and core signals are recorded at different time points of imbibition
- (5) Process and analyze nuclear magnetic resonance data and pseudo-color visualization images

## 4. Result Analysis

**4.1. Core 1.** Figure 4 shows the pseudo-color images generated by scanning of core 1 after being saturated with fluorine oil for 3 days of imbibition, 5 days of imbibition, and 7 days of imbibition. The red area is the area with a strong nuclear

magnetic signal. It can be seen from the evolution of the pseudo-color pictures that as the imbibition time increases, the red area gradually spreads, which indicates that during the process of imbibition, the core and the distilled water in the beaker have a significant fluid replacement. Because the core is placed vertically, the left end of the picture is the upper end of the vertical core. It is not difficult to see that the red area spreads from top to bottom along the core axis, indicating that for core 1, the gravity effect is the most obvious during the self-imbibition process.

Figure 5 shows the corresponding NMR T2 spectrum curve of core 1 saturated with fluorine oil for 3 days of imbibition, 5 days of imbibition, and 7 days of imbibition. From the comparison of the curve differences, it is not difficult to see that the fluid imbibition displacement of core 1 mainly occurs in pore-throat of  $0.25\sim 20\ \mu\text{m}$ , and fluid replacement

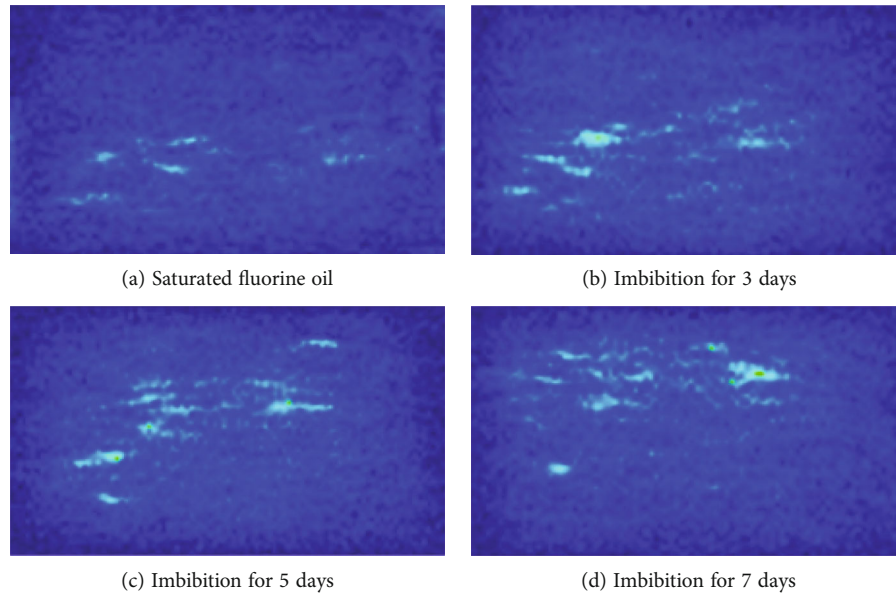


FIGURE 7: Pseudo-color image of core 2 (bright color is the water phase signal).

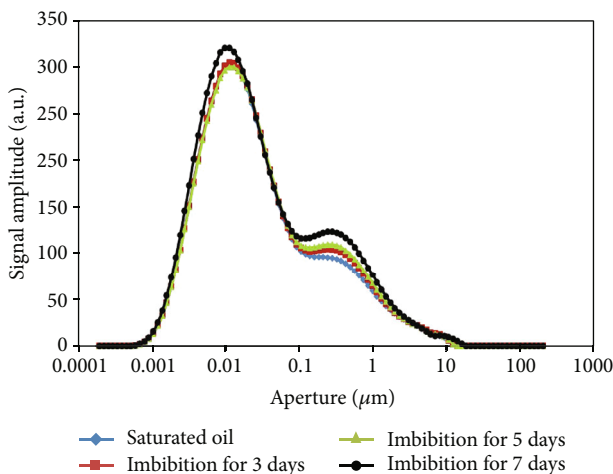


FIGURE 8: NMR T2 spectrum curve of core 2.

of pore throats of  $1.6\sim 10\ \mu\text{m}$  is the most significant. The phenomenon is more obvious in the first 3 days of imbibition replacement, and the efficiency of imbibition replacement is relatively weakened in the next 4 days.

In order to quantitatively characterize the contribution of different types of pore-throat to imbibition oil recovery, the core pore throats are subdivided into four types, including micropores (pore diameter  $\leq 0.025\ \mu\text{m}$ ), pinhole (pore diameter:  $0.025\sim 0.1\ \mu\text{m}$ ), mesopores (pore diameter:  $0.1\sim 1\ \mu\text{m}$ ), and macropores (pore diameter  $> 1\ \mu\text{m}$ ). Figure 6 shows the change curve of water cut of different types of pore-throat of core 1 with time. Statistics show that the total water cut of core 1 increased from 15.31% to 38.37%, and the 168-hour imbibition recovery rate of the core was 23.06%. The macroporous water cut increased from the initial 9.63% to 32.29%, which contributed 98.26% of the total oil production by imbibition; the water cut of mesopores increased from the initial 5.35%

to 5.75%, which contributed 1.73% of the total oil production by imbibition; the contribution of micropores and pinholes was negligible.

4.2. Core 2. Figure 7 shows the pseudo-color images generated by scanning of core 2 after being saturated with fluorine oil for 3 days of imbibition, 5 days of imbibition, and 7 days of imbibition. It can be seen that with the increase in the imbibition time, the bright-colored area diffuses irregularly. Compared with the axial direction of the core, the lateral movement of the fluid is more obvious, which indicates that the capillary force plays a major role in core 2.

Figure 8 shows the corresponding NMR T2 spectrum curve of core 2 saturated with fluorine oil for 3 days of imbibition, 5 days of imbibition, and 7 days of imbibition. From the comparison of the curves, it is not difficult to see that there are mainly two intervals of pore-throat for the fluid imbibition displacement of core 2, namely,  $0.001\sim 0.017\ \mu\text{m}$  interval and  $0.08\sim 2.5\ \mu\text{m}$  interval. The fluid replacement in  $0.08\sim 2.5\ \mu\text{m}$  pore-throat is relatively obvious. What is more, the imbibition replacement is overall stable; the fluid replacement phenomenon is more obvious in the later 2 days. In the first 5 days, the efficiency of imbibition replacement was relatively weakened, indicating that the time of imbibition replacement in cores with poor pore throats was relatively slower.

Figure 9 shows the change curve of water cut of different types of pore-throat of core 2 over time. Statistics show that the total water cut of core 2 increased from 40.42% to 49.33%, and the 168-hour imbibition recovery rate of core 2 was 8.91%. The macroporous water cut increased from the initial 27.81% to 33.63%, contributing 65.35% of the total imbibition oil production; the mesoporous water cut increased from the initial 10.29% to 13.29%, contributing 33.67% of the total imbibition oil production. The contribution of micropores and pinholes are both around 0.5%, and mesopores have been assumed to have more contribution.

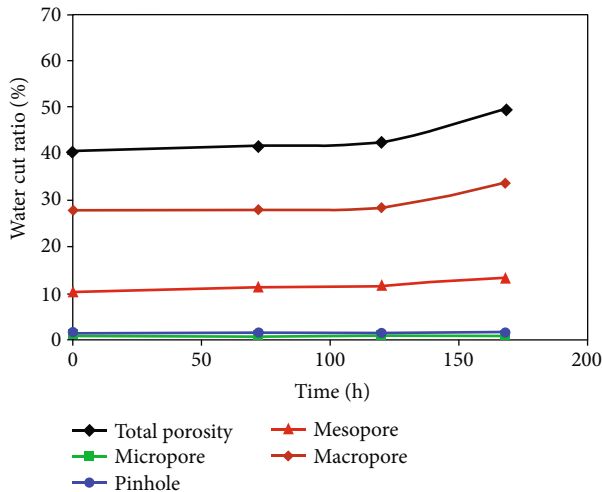


FIGURE 9: Variation curve of water cut of different types of pore-throat in core 2 with imbibition time.

## 5. Conclusions

- (1) For reservoirs with high permeability, gravity is the main controlling force in the process of imbibition. The fluid replacement mainly occurs in the early period of imbibition, and the effect is relatively weak in the later period. Macropores (pore diameter  $> 1 \mu\text{m}$ ) contribute most of the imbibition, and mesopores (pore diameter:  $0.1\sim 1 \mu\text{m}$ ) have a weak contribution. The contribution of micropores and pinholes can be ignored.
- (2) For reservoirs with low permeability, capillary force is the main controlling force in the process of imbibition. The fluid replacement mainly occurs in the later period of imbibition. Early fluid replacement is relatively weak. Macropores (pore diameter  $> 1 \mu\text{m}$ ) contribute most of the imbibition, and mesopores (pore diameter:  $0.1\sim 1 \mu\text{m}$ ) contribute a small part of the imbibition. The contribution of micropores and pinholes can be ignored.
- (3) Regardless of whether the main controlling force is gravity or capillary force, macropores (pore diameter  $> 1 \mu\text{m}$ ) and mesopores (pore diameter  $0.1\sim 1 \mu\text{m}$ ) are the main sources of contribution to imbibition recovery, indicating that oil content and connectivity are two crucial factors that affect imbibition recovery.

## Data Availability

It will be available based on request.

## Conflicts of Interest

The authors declare that they have no conflicts of interest.

## Acknowledgments

The authors would like to acknowledge the National Natural Science Foundation of China (Nos. 51804257, 52004220, 51934005, and 51874242), the Open Fund of State Key Laboratory of Oil and Gas Reservoir Geology and Exploitation (Chengdu University of Technology) (PLC20210316), the PetroChina Innovation Foundation (No. 2020D-5007-0202), and the Innovation and Practice Training Program for Graduate Students (YCS21211006).

## References

- [1] H. Zheng, R. Q. Liao, N. Cheng, and S. Z. Shi, "Microscopic mechanism of fracturing fluid imbibition in stimulated tight oil reservoir," *Journal of Petroleum Science and Engineering*, vol. 202, article 108533, 2021.
- [2] K. Zhang, K. Sebakhy, K. Wu et al., "Future trends for tight oil exploitation," in *SPE 175699, Paper presented at the SPE North Africa Technical Conference and Exhibition*, Cairo, Egypt, September 2015.
- [3] H. L. Chen, L. R. Lucas, L. A. D. Nogaret, H. D. Yang, and D. E. Kenyon, "Laboratory monitoring of surfactant imbibition with computerized tomography," *SPE Reservoir Evaluation and Engineering*, vol. 4, no. 1, pp. 16–25, 2001.
- [4] X. L. Peng, X. Z. Wang, X. Zhou, Z. Y. Lin, F. H. Zeng, and X. L. Huang, "Lab-on-a-chip systems in imbibition processes: a review and applications/issues for studying tight formations," *Fuel*, vol. 306, article 121603, 2021.
- [5] L. Cuice, B. Bourbiaux, and F. Kalaydjian, "Oil recovery by imbibition in low-permeability chalk," *SPE Formation Evaluation (Society of Petroleum Engineers)*, vol. 9, no. 3, pp. 200–208, 1994.
- [6] P. M. Oen, M. E. Jensen, and A. A. Barendregt, "Skjold field, Danish North Sea: early evaluations of oil recovery through water imbibition in a fractured reservoir," *SPE Reservoir Evaluation and Engineering*, vol. 3, no. 1, pp. 17–22, 1988.
- [7] J. Wang, H. Q. Liu, J. Xia et al., "Mechanism simulation of oil displacement by imbibition in fractured reservoirs," *Petroleum Exploration and Development*, vol. 44, no. 5, pp. 805–814, 2017.
- [8] X. Xu, Y. J. Wan, X. Z. Li et al., "Microscopic imbibition characterization of sandstone reservoirs and theoretical model optimization," *Scientific Reports*, vol. 11, no. 1, pp. 8509–8509, 2021.
- [9] S. Liu, J. Ni, X. L. Wen et al., "A dual-porous and dual-permeable media model for imbibition in tight sandstone reservoirs," *Journal of Petroleum Science and Engineering*, vol. 194, article 107477, 2020.
- [10] Z. Y. Wang, H. X. Li, X. M. Lan, K. Wang, Y. F. Yang, and V. Lisitsa, "Formation damage mechanism of a sandstone reservoir based on micro-computed tomography," *Advances in Geo-Energy Research*, vol. 5, no. 1, pp. 25–38, 2021.
- [11] Q. H. Feng, S. Q. Xu, X. D. Xing, W. Zhang, and S. Wang, "Advances and challenges in shale oil development: a critical review," *Advances in Geo-Energy Research*, vol. 4, no. 4, pp. 406–418, 2020.
- [12] H. O. Yildiz, M. Gokmen, and Y. Cesur, "Effect of shape factor, characteristic length, and boundary conditions on spontaneous imbibition," *Journal of Petroleum Science and Engineering*, vol. 53, no. 3-4, pp. 158–170, 2006.

- [13] G. Mason, H. Fischer, N. R. Morrow et al., "Oil production by spontaneous imbibition from sandstone and chalk cylindrical cores with two ends open," *Energy and Fuels*, vol. 24, no. 2, pp. 1164–1169, 2010.
- [14] C. H. Lyu, Z. F. Ning, M. Q. Chen, and Q. Wang, "Experimental study of boundary condition effects on spontaneous imbibition in tight sandstones," *Fuel*, vol. 235, pp. 374–383, 2019.
- [15] Z. M. Yang, X. W. Liu, H. B. Li, Q. H. Lei, Y. T. Luo, and X. Y. Wang, "Analysis on the influencing factors of imbibition and the effect evaluation of imbibition in tight reservoirs," *Petroleum Exploration and Development*, vol. 46, no. 4, pp. 779–785, 2019.
- [16] Y. Jiang, Y. Shi, G. Q. Xu et al., "Experimental study on spontaneous imbibition under confining pressure in tight sandstone cores based on low-field nuclear magnetic resonance measurements," *Energy and Fuels*, vol. 32, no. 3, pp. 3152–3162, 2018.
- [17] A. Habibi, H. Dehghanpour, M. Binazadeh, D. Bryan, and G. Uswak, "Advances in understanding wettability of tight oil formations: a Montney case study," *SPE Reservoir Evaluation and Engineering*, vol. 19, no. 4, pp. 583–603, 2016.
- [18] L. Yang, N. H. Dou, X. B. Lu et al., "Advances in understanding imbibition characteristics of shale using an NMR technique: a comparative study of marine and continental shale," *Journal of Geophysics and Engineering*, vol. 15, no. 4, pp. 1363–1375, 2018.
- [19] A. Bertoncello, J. Wallace, C. Blyton, M. Honarpour, and C. S. S. Kabir, "Imbibition and water blockage in unconventional reservoirs: well-management implications during flowback and early production," *SPE Reservoir Evaluation and Engineering*, vol. 17, no. 4, pp. 497–506, 2014.
- [20] Z. L. Chen, Z. F. Ning, X. F. Yu, Q. Wang, and W. T. Zhang, "New insights into spontaneous imbibition in tight oil sandstones with NMR," *Journal of Petroleum Science and Engineering*, vol. 179, pp. 455–464, 2019.
- [21] L. H. Gao, Z. M. Yang, and Y. Shi, "Experimental study on spontaneous imbibition characteristics of tight rocks," *Advances in Geo-Energy Research*, vol. 2, no. 3, pp. 292–304, 2018.
- [22] F. H. Zeng, Q. Zhang, J. C. Guo, Y. Meng, X. Z. Shao, and Y. J. Zheng, "Capillary imbibition of confined water in nanopores," *Capillarity*, vol. 3, no. 1, pp. 8–15, 2020.
- [23] F. P. Lai, Z. P. Li, T. T. Zhang, A. Q. Zhou, and B. Gong, "Characteristics of microscopic pore structure and its influence on spontaneous imbibition of tight gas reservoir in the Ordos Basin, China," *Journal of Petroleum Science and Engineering*, vol. 172, pp. 23–31, 2019.
- [24] Y. F. Liu, Y. H. Shi, L. Liu, X. C. Yan, D. S. Zhou, and S. Liu, "Determination of the pore-throat limits for water imbibition in tight sandstone reservoirs through NMR analysis," *Journal of Geophysics and Engineering*, vol. 16, no. 1, pp. 253–261, 2019.
- [25] X. P. Li, H. Abass, T. W. Teklu, and Q. Cui, "A shale matrix imbibition model-interplay between capillary pressure and osmotic pressure," in *SPE181407, Paper presented at the SPE Annual Technical Conference and Exhibition*, Dubai, UAE, 2016.
- [26] E. V. Oort, M. Ahmad, R. Spencer, and N. Legacy, "ROP enhancement in shales through osmotic processes," in *SPE/IADC 173138, Paper presented at the Drilling Conference and Exhibition*, London, England, UK, 2015.
- [27] S. Morsy and J. J. Sheng, "Imbibition characteristics of the Barnett shale formation," in *SPE167698, Paper presented at the SPE Unconventional Resources Conference*, Woodlands, Texas, USA, 2014.
- [28] X. Liu, D. S. Zhou, L. Yan, S. Liu, and Y. F. Liu, "On the imbibition model for oil-water replacement of tight sandstone oil reservoirs," *Geofluids*, vol. 2021, Article ID 8846132, 7 pages, 2021.